Research on Chemical Intermediates
https://doi.org/10.1007/s11164-019-03959-1

Optimization of the transfer hydrogenation reaction of acetophenone on Ni@MOF-5 nanoparticles using response surface methodology

Azadeh Nemati Chelavi[1] · Vahid Zare-Shahabadi[1] · Soheil Sayyahi[1] · Hossein Anaraki-Ardakani[1]

Received: 27 June 2019 / Accepted: 23 August 2019

Abstract

In this study, the transfer hydrogenation reduction of acetophenone using supported nickel on MOF as catalyst was investigated. BBD and RSM were employed to investigate the effect of the experimental parameters such as Ni content, catalyst content, temperature, and reaction time. Optimum reaction conditions for the formation of 1-phenylethanol were 45% mol of Ni content, 0.11 g of catalyst, reaction temperature at 83 °C, and reaction time 90 min. The catalyst was characterized by FESEM, EDX, FT-IR, XRD, and H_2-TPR techniques. The catalyst-free reaction phase was analyzed by AAS, and fortunately, no leaching of nickel was detected.

Keywords Transfer hydrogenation · Ni@MOF-5 · Acetophenone · Experimental design

Introduction

Metal–organic frameworks (MOFs) are formed by reticular synthesis [1–3], creating strong bonds between inorganic and organic units [4]. These crystalline materials have been obtained with significant properties such as ultrahigh porosity up to 90% free volume, ultrahigh surface areas up to 10,400 m^2/g, a large pore aperture (98 Å) [5], high mechanical and thermal stability up to < 500 °C in an inert atmosphere and > 350 °C in oxidizing atmospheres, low densities down to 0.13 g/cm^3, and chemical stability in aqueous acid at pH < 0 or in aqueous base at pH > 14 [6]. These properties, along with the extraordinary degree of variability for both the organic and

Electronic supplementary material The online version of this article (https://doi.org/10.1007/s11164-019-03959-1) contains supplementary material, which is available to authorized users.

✉ Soheil Sayyahi
sayyahi.soheil@gmail.com

[1] Department of Chemistry, Mahshahr Branch, Islamic Azad University, Mahshahr, Iran

Published online: 29 August 2019

inorganic components of their structures, have made academic and industrial sectors to be interested in using MOFs for a variety of applications including gas adsorption and storage (like CO_2, H_2, CH_4), catalysis, chemical separations, biomedicine, light harvesting and energy, as well as the degradation of toxic substances such as chemical warfare agents [7–10].

MOFs are considered as dream compounds for catalysis organic reactions and the use of them allows for the combination of the advantages of heterogeneous catalysis (easy post-reaction recovery separation, catalyst reusability, and high stability) and homogeneous catalysis (high efficiency, selectivity, controllability and mild reaction conditions) [5, 11]. The tunability, versatility, high robustness under extreme conditions, high surface areas, and high density of active sites of MOFs offer many advantages regarding their use in catalysis and placing them at the frontier between zeolites and enzymes [12, 13].

In order to take advantage of catalytic behavior, that is, unique to MOFs, it might be necessary to pay more attention to study the application of MOF catalysts in formation reactions of more valuable organic molecules, which can take place under relatively mild conditions [14].

Design and synthesis of MOF-5 ($Zn_4O(BDC)_3$, BDC^{2-} = 1,4-benzenedicarboxylate) was considered as a pioneering work in the chemistry of MOFs [15]. The architectural robustness of MOF-5 allowed for gas adsorption with Brunauer–Emmett–Teller (BET) surface area from 1010 to 4400 m^2/g Langmuir resulting from various preparations methods, with thermal stability of up to 400 °C [16]. These values are substantially higher than those commonly found for zeolites and activated carbon and make MOF-5 suitable candidate in the field of catalysis and gas storage [17].

As an attractive alternative to direct hydrogenation with H_2 gas pressure, transfer hydrogenation (TH) reaction referring to the addition of hydrogen to a molecule from a non-H_2 hydrogen source is a convenient and powerful method to access various hydrogenated compounds. It is an attractive alternative to direct hydrogenation, and it has recently been the interest of many researches in hydrogenation science due to operational simplicity, mild reaction conditions, commercial availability, and environmental friendliness [18]. In recent years, various transition-metal-based catalysts (such as iron, ruthenium, osmium, cobalt, rhodium, iridium, nickel, palladium, and gold) have been applied in both homogenous and heterogeneous systems of TH reactions. In line with this and considering the development and replacement of the more expensive and toxic noble metals, nickel in different forms is found active as catalyst in the reduction of unsaturated compounds with TH methodology [19, 20].

Recently, Lu et al. and Chou et al., in their studies, investigated on the catalytic activity of Ni@MOF-5 for CO_2 methanation at low temperature and for hydrogenation of crotonaldehyde, respectively [21, 22]. In the present chemistry study that is in continuation of our effort to develop new transition-metal-based catalysts [23–25], the results of the MOF-5 catalyzed TH reaction using supported nickel for the reduction of acetophenone to 1-phenylethanol, as an industrial interest compound was reported [19, 26, 27]. Also, experimental design was applied as a powerful tool to get maximum information with minimum number of experiments in order to optimize reaction conditions [28–30].

Results and discussion

In preliminary experiments, it has been shown that when the amounts of loaded Ni (wt%) were more than 45%, the conversion of acetophenone decreased. This might occur due to the surface segregation of Ni particles.

Experimental design

A Box–Behnken design RSM was employed to evaluate the effect of four experimental factors including amount of nickel content (*A*), amount of catalyst (*B*), time of reaction (*C*), and temperature (*D*). These factors were selected as effective experimental variables according to the preliminary studies. A set of 29 experiments was designed using Design Expert software (version 11). Each factor was coded by (−1, 0, +1). The independent factors, their notations, and levels are listed in Table 1.

Using the BBD–RSM experimental design, it was possible to consider a quadratic polynomial regression model to predict the response based on the independent variables. Equation (1) shows the resulted quadratic model.

$$\begin{aligned} \text{Yield} = {} & 13.07 + 3.35A + 4.87B + 1.91C + 1.24D \\ & - 0.45AB + 2.17AC + 3.18AD + 1.20BC \\ & - 3.34BD + 1.15CD - 1.43A^2 - 4.68B^2 - 6.67C^2 - 2.38D^2 \\ & R^2 = 0.75; R^2_{\text{adj}} = 0.50; F = 2.98 \end{aligned} \tag{1}$$

where *A, B, C,* and *D* represent the amount of Ni content, amount of catalyst, reaction time, and temperature, respectively. The product of the reaction was analyzed by GC after each experiment, and the peak area of 1-phenylethanol was considered as response in RSM. The regression sum of squares as a percentage of total sums of squares was equal to 75%, revealing that most portion of variance in the response was explained by the model. Analysis of variance of the quadratic model is presented in Table 2. Table 2 shows that there are some nonsignificant terms in the model that must be removed. Removing all of these terms resulted in the following equation:

$$\begin{aligned} & \text{Yield} = 10.99 + 3.35A + 4.87B - 4.08B^2 - 6.06C^2 \\ & R^2 = 0.58;\ R^2_{\text{adj}} = 0.51; F = 8.21 \end{aligned} \tag{2}$$

The statistics of the model presented in Eq. (2) revealed that the model was not reliable. In order to obtain an empirical equation with a better ability to predict the response, higher order of interactions was considered. In the other words, the main effects along with linear and nonlinear interaction terms of the effective factors were considered as a pool of independent variables. To do so, stepwise method implemented in Design Expert software was employed, and the following regression model was obtained.

Table 1 Independent variables and their levels used in the Box–Behnken design

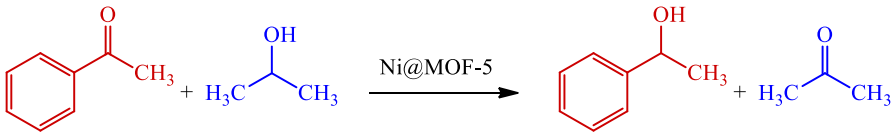

Factors		Level		
		Low	Center	High
		− 1	0	1
Ni content (mol%)		35	40	45
Catalyst content (g)		0	0.1	0.2
Temperature (°C)		70	80	90
Reaction time (min)		30	60	90
Run	*A*	*B*	*C*	*D*	Peak area of 1-phenylethanol
1	1	− 1	0	0	0.04
2	− 1	1	0	0	11.54
3	0	1	1	0	8.53
4	0	1	− 1	0	3.70
5	− 1	0	0	1	7.94
6	− 1	0	1	0	0.07
7	1	0	0	− 1	6.91
8	0	− 1	− 1	0	0.00
9	0	1	0	− 1	19.20
10	0	0	0	0	11.45
11	− 1	− 1	0	0	0.05
12	0	0	0	0	11.87
13	0	1	0	1	5.88
14	− 1	0	0	− 1	2.63
15	− 1	0	− 1	0	0.04
16	0	0	0	0	14.84
17	0	0	0	0	12.65
18	1	0	− 1	0	6.06
19	1	1	0	0	9.74
20	1	0	1	0	14.77
21	0	− 1	0	1	0.04
22	0	0	0	0	14.55
23	0	− 1	1	0	0.03
24	0	0	− 1	− 1	0.02
25	0	0	1	− 1	2.38
26	0	0	− 1	1	0.14

Table 1 (continued)

Run	*A*	*B*	*C*	*D*	Peak area of 1-phenylethanol
27	0	0	1	1	7.11
28	1	0	0	1	24.95
29	0	−1	0	−1	0.01

Table 2 Analysis of variance of the quadratic model

Source	Sum of squares	*df*	Mean square	*F* value	*p* value	
Model	968.26	14	69.16	2.98	0.02	
A–A	134.72	1	134.72	5.81	0.03	
B–B	284.49	1	284.49	12.27	$<1\times10^{-4}$	
C–C	43.79	1	43.79	1.89	0.19	Not significant
D–D	18.54	1	18.54	0.80	0.39	Not significant
AB	0.80	1	0.80	0.03	0.86	Not significant
AC	18.84	1	18.84	0.81	0.38	Not significant
AD	40.50	1	40.50	1.75	0.21	Not significant
BC	5.78	1	5.78	0.25	0.63	Not significant
BD	44.54	1	44.54	1.92	0.19	Not significant
CD	5.31	1	5.31	0.23	0.64	Not significant
A^2	13.33	1	13.33	0.57	0.46	Not significant
B^2	142.19	1	142.19	6.13	0.03	
C^2	288.59	1	288.59	12.45	$<1\times10^{-4}$	
D^2	36.61	1	36.61	1.58	0.23	Not significant
Residual	324.59	14	23.19			
Lack of fit	315.03	10	31.50	13.18	0.01	Significant
Pure error	9.56	4	2.39			

$$\begin{aligned}\text{Yield} = {} & +13.15 + 5.25A + 5.78B + 1.91C + 2.17AC + 3.18AD - 3.34BD - 3.15B^2 \\ & - 7.47C^2 - 3.17D^2 + 5.84A^2D - 5.70AB^2 - 3.32B^2D - 2.73BC^2 - 4.65A^2B^2 \\ R^2 = 0.97;\ & R^2_{\text{adj}} = 0.94; F = 33.96\end{aligned} \tag{3}$$

The results of the squared correlation coefficient of the model and other statistical parameters presented in Eq. (3) showed that the resulting model was reliable and can be used to quantitatively and accurately predict the response. Analysis of variance of the model is also presented in Table 3. It was found that all terms were significant with high *F* values and low *P* values. The *F* value of the model was equal to 33.96 (compared to the critical value of 2.48 at the 0.05 level of significance) with a *P* value of less than 3×10^{-8}. In order to test whether the data set is normally distributed, the normal probability plot of residuals is drawn and, and it is depicted in Fig. 1. Figure 1 shows that the points fell close enough to the straight line and

Table 3 Analysis of variance of the model shown in Eq. 3

Source	Sum of squares	*df*	Mean square	*F* value	*P* value	
Model	1255.88	14	89.71	33.96	$<1\times10^{-4}$	Significant
A–A	220.61	1	220.61	83.52	$<1\times10^{-4}$	
B–B	267.08	1	267.08	101.12	$<1\times\times10^{-4}$	
C–C	43.79	1	43.79	16.58	0.001	
AC	18.84	1	18.84	7.13	0.018	
AD	40.50	1	40.50	15.33	0.002	
BD	44.54	1	44.54	16.86	0.001	
B^2	53.99	1	53.99	20.44	0.001	
C^2	319.85	1	319.85	121.10	$<1\times10^{-4}$	
D^2	57.75	1	57.75	21.86	0.001	
A^2D	136.31	1	136.31	51.61	$<1\times10^{-4}$	
AB^2	86.69	1	86.69	32.82	$<1\times10^{-4}$	
B^2D	44.12	1	44.12	16.70	0.001	
BC^2	19.83	1	19.83	7.51	0.016	
A^2B^2	44.44	1	44.44	16.82	0.001	
Residual	36.98	14	2.64			
Lack of fit	27.41	10	2.74	1.15	0.49	Not significant
Pure error	9.56	4	2.39			

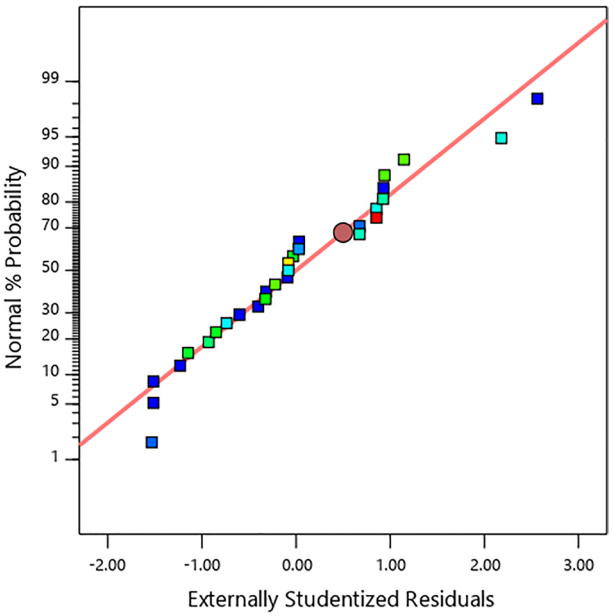

Fig. 1 Normal probability plot of residuals of the model presented in Eq. 3

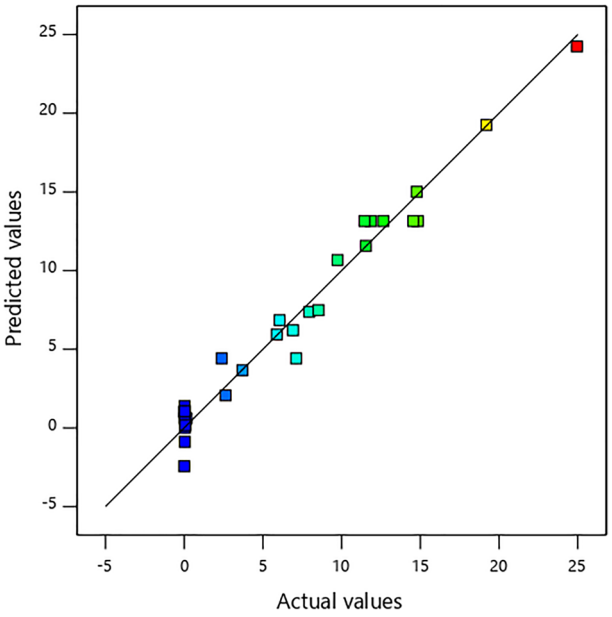

Fig. 2 Predicted values versus actual values for peak area of 1-phenylethanol of TH reaction of acetophenone

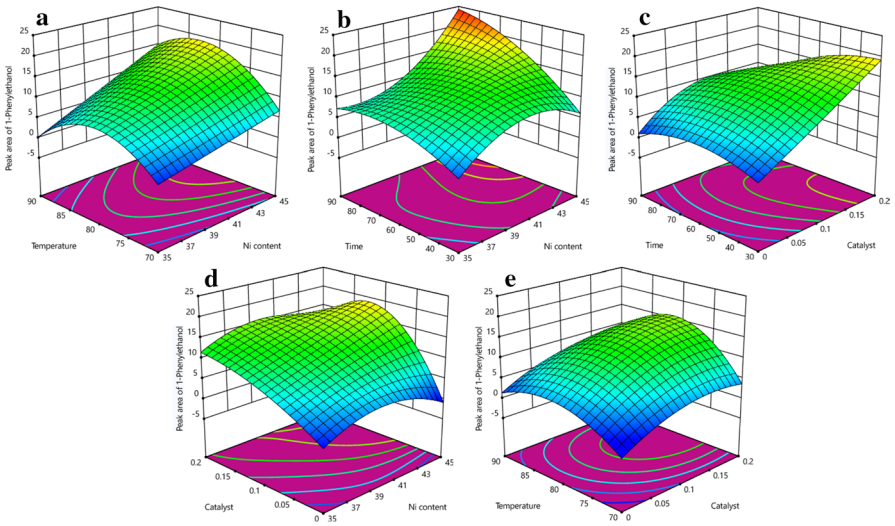

Fig. 3 Response surface plots **a** *A*–*C*; **b** *A*–*D*; **c** *B*–*D*; **d** *A*–*B*; and **e** *B*–*C*

passed through the center of the plot. As a result, the experimental points followed a straight line suggesting normal distribution in the data. A plot related to the predicted response versus actual values is shown in Fig. 2. It is clear that the data points

were well distributed close to a straight line with squared correlation coefficient of 0.971.

Figure 3 shows response surface plots, which are useful to evaluate interaction between two independent variables while keeping the others' value as constant. Such three-dimensional plots provide valuable information about behavior of the system. Figure 3a shows the interaction of Ni content of catalyst with reaction temperature and their relation with peak area of 1-phenylethanol of the TH reaction. It is well known that the temperature is regarded as a very important parameter in chemical reactions. Figure 3a shows that, in the reaction system, the maximum product was formed at about 80 °C. In the other words, as temperature increases, the conversion of the TH reaction increases, but at temperatures above 80 °C, the conversion decreases due to the steady evaporation of acetophenone. The progress of the TH reaction in the presence of the catalyst with different amounts of Ni content is depicted in Fig. 3b. Figure 3b shows that the progress of the TH reaction in the presence of catalyst with lower amount of Ni content was not satisfactory. The yield of the reaction increases as the reaction time increases, when the catalyst with higher load of nickel is used. In the other words, in the presence of the catalyst with lower Ni content than 35%, the reaction does not proceed considerably. Figure 3c shows the interaction of amount of catalyst with reaction time and their relation with the amount of 1-phenylethanol. It should be mentioned that the lower amount of catalyst used in the experimental design was equal to 0.0 g, to check whether the reaction proceeds in the absence of the catalyst. Figure 3c shows that the reaction did not proceed considerably in the absence of the catalyst. The interaction of Ni content with amount of catalyst and their relation with the response is shown in Fig. 3d. The regression coefficients of two terms responsible to the interaction between factors A and B (e.g., AB^2, A^2B^2) were found to be significant and large compared to the main effects of these factors. Some extent of curvature of the graph occurred due to higher order of terms and interactions used in development of the model. Nevertheless, Fig. 3d shows that the yield of the reaction was low in the absence of the catalyst and/or in the presence of the catalyst with lower Ni contents. The interaction between catalyst amount and reaction temperature is displayed in Fig. 3e. The trend in this figure was found to be similar to that in Fig. 3a. Optimal conditions to get the highest amount of 1-phenylethanol were determined based on the investigation of the profile of the desirable response, and they are depicted in Fig. S1. The desirability value corresponding to the maximum peak area of the product of the TH reaction was equal to 0.997 with the peak area of 24.88. This high product yield was obtained provided that experimental conditions were set as: 45% mol of Ni content, 0.11 g of catalyst, at the temperature of 83 °C, and at 90 min of reaction time. The average peak area at this optimum condition was about 24.8%.

Characterization of catalyst

Characterization of the catalyst was done using various techniques including FESEM, EDX, FT-IR, and XRD.

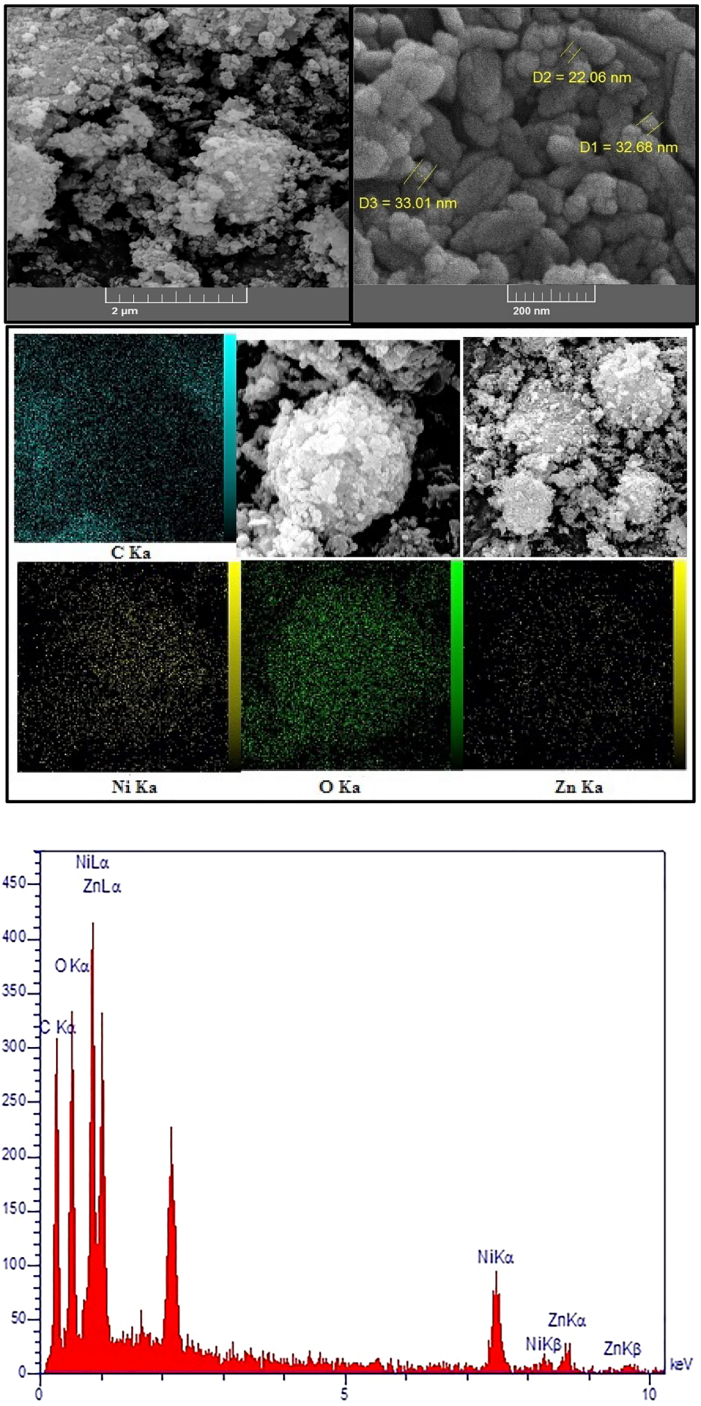

Fig. 4 FESEM images and SEM–EDS elemental mapping images of C, Ni, O, and Zn in 45Ni@MOF-5 (up); EDX of 45Ni@MOF-5 (down)

Fortunately, Fig. 4 shows the elemental mapping, indicating that nickel (Yellow) has a good distribution over the surface of the catalyst, and the average size of the particles is from about 22 to 33 nm with almost uniform shape. Besides, the EDS spectrum shows signals clearly confirming the presence of Ni in addition to C, O, and Zn.

The FT-IR spectra of guest-free MOF-5 and 45Ni@MOF-5 are shown in Fig. S2. Figure S2 shows that almost all bonds shifted after the loading of MOF-5 with Ni. For example, the strong band belonging to the C=O stretching vibration of carboxylate anions appeared at ~ 1554 cm^{-1} and ~ 1583 cm^{-1} for MOF-5 and 40Ni@MOF-5, respectively. In the case of 40Ni@MOF-5, a strong band appeared at ~ 1381 cm^{-1} was associated with the carboxyl group symmetric stretching, and bonds appeared at ~ 1016 cm^{-1}, ~ 825 cm^{-1}, and ~ 684 cm^{-1} were ascribed to the out of plane vibrations of the BDC linker [31]. Also, the broadbands appeared at ~ 3440 cm^{-1} to ~ 3608 cm^{-1} were attributed to the presence of water in the metal coordination sphere [32].

The analysis of XRD pattern revealed information about the crystallographic structure, chemical composition, and physical properties of the catalyst [33]. The XRD pattern of 45Ni@MOF-5 catalyst, MOF-5, and simulated pattern are presented in Fig. 5. Figure 5 shows the characteristic peaks in the 2θ region of 0–80°, indicating that they were matched well compared to the corresponding standard and similar reported pattern (JCPDS no. 87-0712) [21]. A very sharp peak at $2\theta = 8.99$ indicated the high crystallinity of MOF-5 based on the catalyst. Additionally, peaks

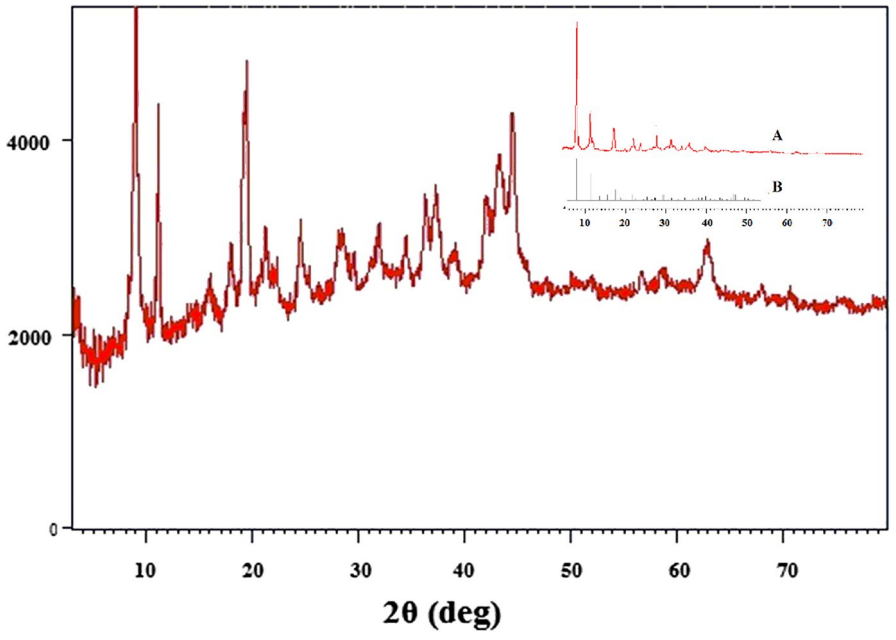

Fig. 5 XRD pattern of 45Ni@MOF-5; MOF-5 (A) and simulated (B) patterns

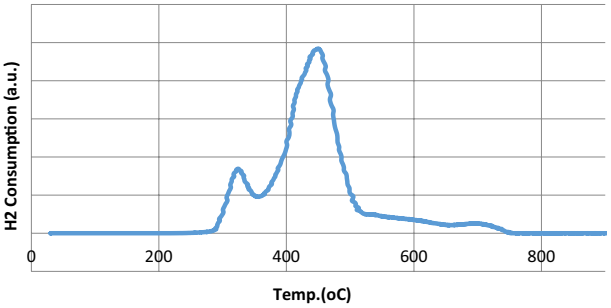

Fig. 6 H_2-TPR profile of 45Ni@MOF-5

at $2\theta = 44.52$, 51.91, and 75.48 were assigned to metallic Ni with a face-centered cubic structure.

The TPR technique is used to study the reducibility of supported nickel catalysts [34–36]. A number of factors such as the amount of Ni loading, catalyst preparation protocol, and interaction between Ni ions and supports have proven to affect the reducibility [37]. Figure 6 shows the H_2-TPR profile for 45Ni@MOF-5 from 30 to 900 °C. It indicates that there are two hydrogen consumption peaks: a small one at around 322 °C and a broad one at around 450 °C which can be attributed to the reduction of Ni species at surface and within frameworks of the catalyst, respectively.

Experimental section

General

All chemicals were purchased from commercial sources and were used right after reception. Progress of reactions was followed by gas chromatographic (GC) analyses and was performed using a DANI GC equipped with a flame ionization detector (FID) and a column (length = 150 m, inner diameter = 0.25 mm, and film thickness = 1.00 μm). The Fourier transform infrared (FT-IR) spectra (ν_{max}) were measured as a KBr disk using a BOMEM MB-Series 1998 FT-IR spectrometer and at a scanning range of 4000–400 cm^{-1}. Scanning electron microscopy (SEM) analyses were performed on a Tescan Mira 3 LMU instrument coupled with energy-dispersive X-ray (EDX) spectroscopy at a potential of 15 kV with 1-nm resolution for microanalysis and mapping of the catalyst. X-ray powder diffraction (XRD) was applied for obtaining the XRD patterns of samples using Cu Kα radiation source on a PANalytical X-ray diffractometer Model X'Pert Pro. The H_2 temperature-programmed reduction (H_2-TPR) experiments were performed on a NanoSORD NS91 apparatus (Sensiran Co. Ltd., Tehran, Iran) equipped with a thermal conductivity detector (TCD).

Synthesis of the Ni@MOF-5

MOF-5 was synthesized using an optimized procedure starting with the use of terephthalic acid, zinc nitrate, and diethylformamide as organic solvents [9]. Ni@MOF-5 catalysts were prepared by a modified procedure of impregnation methods according to the previous studies [21]. A mixture of Ni (acac) $_2$ (1.71 g, 6.6 mmol) was magnetically stirred in ethanol (250 mL) and was heated at 60 °C. MOF-5 (1.8 g) was added to the obtained dark green solution, and the resulted mixture was heated for 16 h. Then, hydrazine solution (5 mL, 80 wt%) was added to the mixture and was heated for another 6 h. The ensuing mixture was filtered, was washed with water (5 × 10 mL), then was dried at 110 °C for 12 h, and was calcined at 250 °C under an air atmosphere for 5 h to obtain the final product.

Catalytic study

The activities of the catalysts with different amounts of Ni content were measured based on the results obtained from the transfer hydrogenation of acetophenone. All experiments were carried out in a Teflon-lined autoclave. Typically, a mixture of acetophenone (0.12 g, 1 mmol), 2-propanol (4 mL), and specified amount of the catalyst were transferred into the Teflon-lined autoclave and were treated for predefined reaction time at specified temperature. Then, the catalyst was filtered off, and the progress of the reactions was analyzed by gas chromatograph. The type and amount of the catalyst, time, and temperature of reaction were considered as those experimental factors influencing the reaction conversion of acetophenone to 1-phenylethanol, and, therefore, they were studied by experimental design in details.

The reusability and leaching of the catalyst is a great concern for most of the supported catalyst. In this regard, the catalyst was recovered, was washed with ethanol for several times, then was dried at 110 °C in an oven, and then it was reused. Fortunately, the catalyst did not show significant loss in activity after five runs. The catalyst-free reaction phase was also analyzed by atomic absorption spectroscopy, and the amount of <2 ppm of nickel was found.

Experimental design and optimization

In order to investigate the effect of the experimental parameters on the transfer hydrogenation reaction yield for acetophenone, Box–Behnken experimental design (BBD) and response surface methodology (RSM) were employed. Compared to the one-factor-at-a-time method, the use of RSM design reduces the number of experiments required to determine the effect of understudied factors.

Box–Behnken design (BBD) is a spherical, rotatable, or nearly rotatable quadratic RSM design. It is done based on a three-level fractional factorial design including the central point and middle points of the edges. The number of experimental runs (N) was calculated by the following formula: $N = 2k(k-1) + C_p$, where k represents the number of variables and C_p represents the number of center points [38]. The factors selected for the optimization of reaction yield included amount of loaded nickel, amount of catalyst, time of reaction, and temperature. Peak area of the

product, e.g., 1-phenylethanol, was considered as the response or dependent variable to be measured in relation to the conversion in the reaction. BBD experiments were designed using Design Expert software (version 11), and experiments were performed in randomized order. The central point was replicated five times to obtain a good estimation of random errors. Empirical equation relating response to the independent variables was generated in Design Expert environment. The same software was used to extract response surface plots and to predict optimum conditions. The actual and coded values of each factor are presented in Table 2. A preliminary study was carried out to select the levels of each factor. The lower amount of the catalyst was equal to 0.0 g, which was used to monitor the progress of the reaction in the absence of the catalyst. The upper limit of catalyst amount, e.g., 0.2 g, was determined according to the preliminary study. Results showed that higher amount of the catalyst caused a significant decrease in the formation of the product in the TH reaction of acetophenone, which may occur due to the catalyst agglomeration. Limits of Ni contents were assigned to be between 35 and 45 wt%, respectively, since the preliminary study indicated that insignificant amount of conversion was obtained outside of this range.

Conclusion

In this study, an extensive experimental design and surface response method were used to study the effective parameters such as Ni content, catalyst amount, reaction temperature, and time on the synthesis of 1-phenylethanol catalyzed by Ni-MOF nanoparticles through TH reduction. Also, the interaction of variables was evaluated with the least number of possible tests. According to the statistical analysis, the best obtained results belonged to the catalyst loaded with 45% of Ni.

Acknowledgements We gratefully acknowledge the funding support received for this project from the Mahshahr Branch, Islamic Azad University, Iran.

References

1. O.M. Yaghi, M. O'Keeffe, N.W. Ockwig, H.K. Chae, M. Eddaoudi, J. Kim, Nature **423**, 705 (2003)
2. J.L.C. Rowsell, O.M. Yaghi, Microporous Mesoporous Mater. **73**, 3 (2004)
3. Y. Liu, M. O'Keeffe, M.M.J. Treacy, O.M. Yaghi, Chem. Soc. Rev. **47**, 4642 (2018)
4. H. Furukawa, K.E. Cordova, M. O'Keeffe, O.M. Yaghi, Science **341**, 1230444 (2013)
5. A.H. Chughtai, N. Ahmad, H.A. Younus, A. Laypkov, F. Verpoort, Chem. Soc. Rev. **44**, 6804 (2015)
6. A.J. Howarth, Y. Liu, P. Li, Z. Li, T.C. Wang, J.T. Hupp, O.K. Farha, Nat. Rev. Mater. **1**, 15018 (2016)
7. H.-C. Zhou, J.R. Long, O.M. Yaghi, Chem. Rev. **112**, 673 (2012)
8. P. Silva, S.M.F. Vilela, J.P.C. Tomé, F.A.A. Paz, Chem. Soc. Rev. **44**, 6774 (2015)
9. U. Mueller, M. Schubert, F. Teich, H. Puetter, K. Schierle-Arndt, J. Pastré, J. Mater. Chem. **16**, 626 (2006)
10. D. Wang, Z. Li, Res. Chem. Intermed. **43**, 5169 (2017)

11. D. Burrows Andrew, K. Cadman Laura, J. Gee William, H. Amer Hamzah, V. Knichal Jane, and S. Rochat, *Tuning the Properties of Metal–Organic Frameworks by Post-synthetic Modification*, ed. by H. García and S. Navalón. Metal–organic frameworks. Wiley (2018)
12. F. David, A. Sonia, P. Catherine, Angew. Chem. Int. Ed. **48**, 7502 (2009)
13. J. Lee, O.K. Farha, J. Roberts, K.A. Scheidt, S.T. Nguyen, J.T. Hupp, Chem. Soc. Rev. **38**, 1450 (2009)
14. J. Liu, L. Chen, H. Cui, J. Zhang, L. Zhang, C.-Y. Su, Chem. Soc. Rev. **43**, 6011 (2014)
15. H. Li, M. Eddaoudi, M. O'Keeffe, O.M. Yaghi, Nature **402**, 276 (1999)
16. S.S. Kaye, A. Dailly, O.M. Yaghi, J.R. Long, J. Am. Chem. Soc. **129**, 14176 (2007)
17. T. Segakweng, N.M. Musyoka, J. Ren, P. Crouse, H.W. Langmi, Res. Chem. Intermed. **42**, 4951 (2016)
18. D. Wang, D. Astruc, Chem. Rev. **115**, 6621 (2015)
19. K. Vijayakrishna, K.T.P. Charan, K. Manojkumar, S. Venkatesh, N. Pothanagandhi, A. Sivaramakrishna, P. Mayuri, A.S. Kumar, B. Sreedhar, ChemCatChem **8**, 1139 (2016)
20. F. Alonso, P. Riente, M. Yus, Acc. Chem. Res. **44**, 379 (2011)
21. W. Zhen, B. Li, G. Lu, J. Ma, Chem. Commun. **51**, 6556 (2015)
22. H. Zhao, H. Song, L. Chou, Inorg. Chem. Commun. **15**, 261 (2012)
23. F.K. Olia, S. Sayyahi, N. Taheri, C. R. Chim. **20**, 370 (2017)
24. S. Sayyahi, S. Mozafari, S.J. Saghanezhad, Res. Chem. Intermed. **42**, 511 (2016)
25. A. Shouli, S. Menati, S. Sayyahi, C. R. Chim. **20**, 765 (2017)
26. R. Molinari, C. Lavorato, P. Argurio, Chem. Eng. J. **274**, 307 (2015)
27. B. Zhang, F. Xie, J. Yuan, L. Wang, B. Deng, Catal. Commun. **92**, 46 (2017)
28. C.A. McNamara, F. King, M. Bradley, Tetrahedron Lett. **45**, 8239 (2004)
29. H. Naeimi, V. Nejadshafiee, S. Masoum, Appl. Organomet. Chem. **29**, 314 (2015)
30. M. Ghiassee, M. Rezaei, F. Meshkani, S. Mobini, Res. Chem. Intermed. **45**, 4501 (2019)
31. M. Zhang, J. Guan, B. Zhang, D. Su, C.T. Williams, C. Liang, Catal. Lett. **142**, 313 (2012)
32. N.T.S. Phan, K.K.A. Le, T.D. Phan, Appl. Catal. A **382**, 246 (2010)
33. R.K. Sharma, Y. Monga, A. Puri, J. Mol. Catal. A Chem. **393**, 84 (2014)
34. Y. Jiang, T. Huang, Y. Xu, X. Li, Z. Qin, H. Ji, Chem. Eng. Technol. **41**, 175 (2018)
35. T.A. Le, M.S. Kim, S.H. Lee, T.W. Kim, E.D. Park, Catal. Today **293–294**, 89 (2017)
36. D.V. Peron, V.L. Zholobenko, M.R. de la Rocha, M. Oberson de Souza, L.A. Feris, N.R. Marcilio, V.V. Ordomsky, A.Y. Khodakov, J. Mater. Sci. **54**, 5399 (2019)
37. A. Parmaliana, F. Arena, F. Frusteri, N. Giordano, J. Chem. Soc. Faraday Trans. **86**, 2663 (1990)
38. N. Chamkouri, A. Niazi, V. Zare-Shahabadi, Spectrochim Acta A Mol Biomol Spectrosc **156**, 105 (2016)